ELECTRON-CAPTURE SUPERNOVAE AS THE ORIGIN OF ELEMENTS BEYOND IRON

Shinya Wanajo[1, 2], Hans-Thomas Janka[2], and Bernhard Müller[2]

Draft version September 7, 2010

ABSTRACT

We examine electron-capture supernovae (ECSNe) as sources of elements heavier than iron in the solar system and in Galactic halo stars. Nucleosynthesis calculations are performed on the basis of thermodynamic histories of mass elements from a fully self-consistent, two-dimensional (2D) hydro-dynamic explosion model of an ECSN. We find that neutron-rich convective lumps with an electron fraction down to $Y_{e,min} = 0.40$, which are absent in the one-dimensional (1D) counterpart, allow for interesting production of elements between the iron group and $N = 50$ nuclei (from Zn to Zr, with little Ga) in nuclear statistical equilibrium and by the α-process. Our models yield very good agreement with the Ge, Sr, Y, and Zr abundances of r-process deficient Galactic halo stars and constrain the occurrence of ECSNe to ∼4% of all stellar core-collapse events. If tiny amounts of additional material with slightly lower $Y_{e,min}$ down to ∼0.30–0.35 were also ejected —which presently cannot be excluded because of the limitations of resolution and two-dimensionality of the model—, a weak r-process can yield elements beyond $N = 50$ up to Pd, Ag, and Cd as observed in the r-process deficient stars.

Subject headings: nuclear reactions, nucleosynthesis, abundances — stars: abundances — stars: neutron — supernovae: general

1. INTRODUCTION

Electron-capture supernovae (ECSNe) have been proposed as possible origin of elements beyond iron, in particular of heavy r-process elements. This is due to the distinctive features of the collapsing O-Ne-Mg cores (Nomoto 1987). The cores with their fairly small mass (∼$1.38\,M_\odot$), steep surface density gradient, and dilute H/He envelope (in the super-asymptotic-giant-branch or SAGB stage) were expected to enable prompt explosions, where the ejection of neutron(n)-rich matter with an electron fraction (number of protons per baryon) of $Y_e \approx 0.14$ could be possible (Wanajo et al. 2003). Chemical evolution studies also favor ECSNe at the lower end (∼8–$10\,M_\odot$) of the mass range of core-collapse supernovae (CCSNe) to account for the abundance signatures of Galactic halo stars (Ishimaru & Wanajo 1999).

Recent one-dimensional (1D) hydrodynamic simulations of O-Ne-Mg core collapse with elaborate neutrino transport, however, found delayed neutrino-driven explosions (Kitaura, Janka, & Hillebrandt 2006). This result was confirmed by Dessart et al. (2006) and excludes the prompt explosions of Hillebrandt et al. (1984). The shocked surface layers of the O-Ne-Mg core are also far from the r-process conditions envisioned by Ning et al. (2007) as shown by Janka et al. (2008).

Detailed nucleosynthesis studies based on the 1D results of Kitaura, Janka, & Hillebrandt (2006), however, suggest that ECSNe can be the source of nuclei up to $N = 50$, in particular of Zn and light p-nuclei (up to ^{92}Mo), whose origins are not fully understood (see also Hoffman et al. 2008). Wanajo et al. (2009) further speculated that the nucleosynthetic outcome could be considerably altered in the multi-dimensional case.

Spectroscopic studies of Galactic halo stars indicate the presence of a significant fraction of r-process *deficient* Galactic halo stars that possess high Sr-Y-Zr ($N = 50$) abundances relative to heavy r-process material (Johnson & Bolte 2002; Honda et al. 2006). This implies the contribution from an astrophysical source making $N = 50$ species without heavy r-process elements (Travaglio et al. 2004; Wanajo & Ishimaru 2006; Qian & Wasserburg 2008). Recently Arcones and Montes (2010), employing trajectories from 1D hydrodynamic models and varying the corresponding Y_e, proposed that the baryonic wind blown off the surface of new-born ("proto-") neutron stars (PNSs) by neutrino heating could be production sites of such nuclei in the early Galaxy.

New 2D explosion simulations of ECSNe exhibit n-rich lumps of matter being dredged up by convective overturn from the outer layers of the PNS during the early stages of the explosion (§ 2; Müller, Janka, & Kitaura, in preparation), a feature that is absent in the 1D situation. In this *Letter* we present the first nucleosynthesis study on the basis of such self-consistent 2D models. Without invoking any free parameters we show that ECSNe could be an important source of the elements between the iron peak and the $N = 50$ region in the Sun and the early Galaxy, perhaps even of light r-process nuclei up to Cd.

2. TWO-DIMENSIONAL SUPERNOVA MODEL

The nucleosynthesis analysis made use of about 2000 representative tracer particles, by which the thermodynamic history of ejecta chunks was followed in our 2D hydrodynamic calculation of an ECSN. The model was computed with a sophisticated (ray-by-ray-plus) treatment of the energy-dependent neutrino transport, using the Prometheus-Vertex code and the same microphysics (weak-interaction rates, nuclear burning treatment, and nuclear equation of state of Lattimer & Swesty 1991) as in its 1D counterpart (Kitaura, Janka, & Hillebrandt 2006). Some aspects of

[1] Technische Universität München, Excellence Cluster Universe, Boltzmannstr. 2, D-85748 Garching, Germany; shinya.wanajo@universe-cluster.de

[2] Max-Planck-Institut für Astrophysik, Karl-Schwarzschild-Str. 1, D-85748 Garching, Germany; thj@mpa-garching.mpg.de
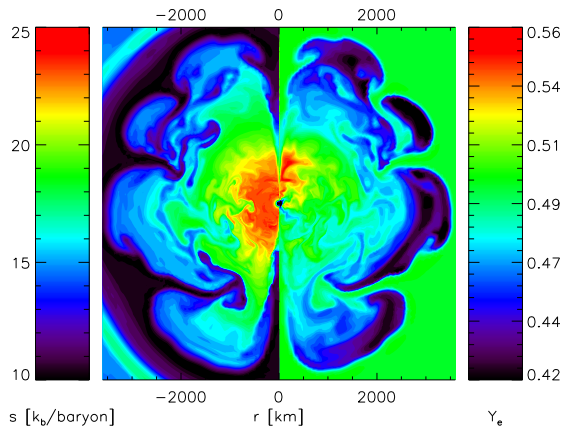
FIG. 1.— Snapshot of the convective region of the 2D simulation of an ECSN at 262 ms after core bounce with entropy per nucleon (s; left) and Y_e (right). Mushroom-shaped lumps of low-Y_e matter are ejected during the early phase of the explosion.
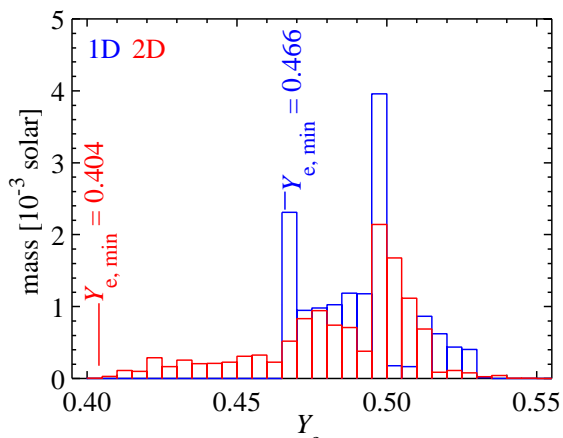

FIG. 2.— Ejecta masses vs. Y_e for the 1D (blue) and 2D (red) explosion models. The width of a Y_e-bin is chosen to be $\Delta Y_e = 0.005$. The minimum values of Y_e are indicated for both cases.
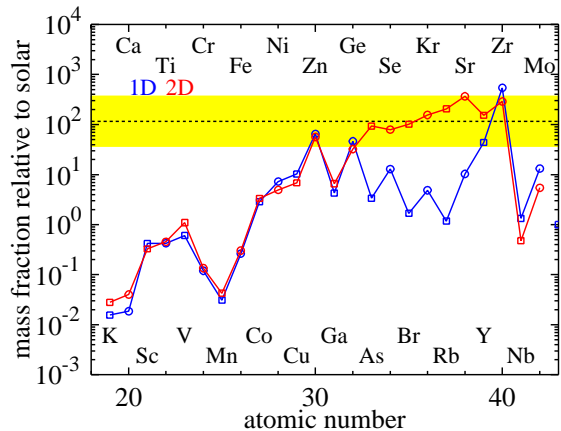

FIG. 3.— Elemental mass fractions in the ECSN ejecta relative to their solar values (Lodders 2003), comparing the 2D results (red) with the 1D counterpart (blue) from Wanajo et al. (2009). Even-Z and odd-Z elements are denoted by circles and squares, respectively. The normalization band (see text) is marked in yellow.
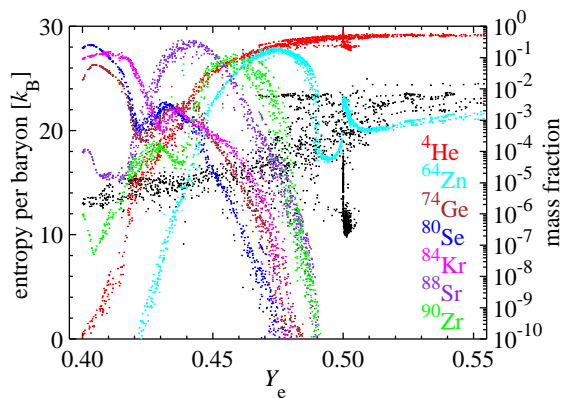

FIG. 4.— Mass fractions of the dominant isotopes of the even-Z elements vs. Y_e for all investigated thermodynamic trajectories. Also shown are the mass fractions of ^{4}He (α-particles) (red) and the entropies of the trajectories (black dots, left vertical axis).

the 2D model in comparison to 1D results were discussed by Janka et al. (2008), and a more complete description can be found in a separate publication (Müller et al., in preparation).

The pre-collapse model of the O-Ne-Mg core emerged from the evolution of an $8.8\,M_\odot$ star (Nomoto 1987). Because of the very steep density gradient near the core surface, the shock expands continuously, and a neutrino-powered explosion sets in at $t \sim 100\,\mathrm{ms}$ p.b. in 1D and 2D essentially in the same way and with a very similar energy ($\sim 10^{50}\,\mathrm{erg}$; Janka et al. 2008).

In the multi-dimensional case, however, the negative entropy profile created by neutrino heating around the PNS leads to a short phase of convective overturn, in which accretion downflows deleptonize strongly, are neutrino heated near the neutrinosphere, and rise again quickly, accelerated by buoyancy forces. Thus n-rich matter with modest entropies per nucleon ($s \sim 13$–$15\,k_\mathrm{B}$; k_B is Boltzmann's constant) gets ejected in mushroom-shaped structures typical of Rayleigh-Taylor instability. Figure 1 displays the situation 262 ms after bounce when the pattern is frozen in and self-similarly expanding.

As a consequence, the mass distribution of the ejecta in the 2D model extends down to $Y_{e,\mathrm{min}}$ as low as ~ 0.4, which is significantly more n-rich than in the correspond-

ing 1D case ($Y_{e,\mathrm{min}}^{1D} \sim 0.47$)[3]. Figure 2 shows the Y_e-histograms at the end of the simulations. The total ejecta masses are $1.39 \times 10^{-2}\,M_\odot$ for the 1D model and $1.14 \times 10^{-2}\,M_\odot$ in 2D, where the difference is partly due to the different simulation times, being $\sim 800\,\mathrm{ms}$ and $\sim 400\,\mathrm{ms}$, respectively (core bounce occurs at $\sim 50\,\mathrm{ms}$). However, the ejecta after $\sim 250\,\mathrm{ms}$ p.b. are only proton-rich, contributing merely to the $Y_e > 0.5$ side in Fig. 2.

3. NUCLEOSYNTHESIS FOR THE ECSN MODEL

The nucleosynthetic yields are obtained with the reaction network code (including neutrino interactions) described in Wanajo et al. (2009). Using thermodynamic trajectories directly from the 2D ECSN model, the calculations are started when the temperature decreases to $9 \times 10^9\,\mathrm{K}$, assuming initially free protons and neutrons with mass fractions Y_e and $1 - Y_e$, respectively. The final abundances for all isotopes are obtained by mass-integration over all 2000 marker particles.

---

[3] Note that the exact lower bound of the mass distribution vs. Y_e in the 1D case is highly sensitive to details of the neutrino transport, e.g. the number and interpolation of grid points in energy space. In a recent simulation with improved spectral resolution, Hüdepohl et al. (2010) obtained $Y_{e,\mathrm{min}} = 0.487$.

The resulting *elemental* mass fractions relative to solar values (Lodders 2003), or the production factors, are shown in Fig. 3 (red) compared to the 1D case (blue) from Wanajo et al. (2009). The "normalization band" between the maximum (367 for Sr) and a tenth of that is indicated in yellow with the medium marked by a dotted line. The total ejecta mass is taken to be the sum of the ejected mass from the core and the outer H/He-envelope ($= 8.8\,M_\odot - 1.38\,M_\odot + 0.0114\,M_\odot = 7.43\,M_\odot$). Note that the $N = 50$ species, ^{86}Kr, ^{87}Rb, ^{88}Sr, and ^{90}Zr, have the largest production factors for *isotopes* with values of 610, 414, 442, and 564, respectively.

As discussed by Wanajo et al. (2009), in the 1D case only Zn and Zr are on the normalization band, although some light p-nuclei (up to ^{92}Mo) can be sizably produced. In contrast, we find that all elements between Zn and Zr, except for Ga, fall into this band in the 2D case (Ge is marginal), although all others are almost equally produced in 1D and 2D. This suggests ECSNe to be likely sources of Zn, Ge, As, Se, Br, Kr, Rb, Sr, Y, and Zr, in the Galaxy. Note that the origin of these elements is not fully understood, although Sr, Y, and Zr in the solar system are considered to be dominantly made by the s-process. The ejected masses of ^{56}Ni ($\rightarrow^{56}$Fe; $3.0 \times 10^{-3}\,M_\odot$) and all Fe ($3.1 \times 10^{-3}\,M_\odot$) are the same as in the 1D case ($2.5 \times 10^{-3}\,M_\odot$, Wanajo et al. 2009).

The fact that oxygen is absent in ECSN ejecta but a dominant product of more massive CCSNe, can pose a constraint on the frequency of ECSNe (Wanajo et al. 2009). Considering the isotope ^{86}Kr with its largest production factor in our 2D model and assuming f to be the fraction of ECSNe relative to all CCSNe, one gets

$$\frac{f}{1-f} = \frac{X_\odot(^{86}\text{Kr})/X_\odot(^{16}\text{O})}{M(^{86}\text{Kr})/M_{\text{noEC}}(^{16}\text{O})} = 0.050, \qquad (1)$$

where $X_\odot(^{86}\text{Kr}) = 2.4 \times 10^{-8}$ and $X_\odot(^{16}\text{O}) = 6.6 \times 10^{-3}$ are the mass fractions in the solar system (Lodders 2003), $M(^{86}\text{Kr}) = 1.1 \times 10^{-4}\,M_\odot$ is our ejecta mass of ^{86}Kr, and $M_{\text{noEC}}(^{16}\text{O}) = 1.5\,M_\odot$ the production of ^{16}O by all other CCSNe, averaged over the stellar initial mass function between $13\,M_\odot$ and $40\,M_\odot$ (see Wanajo et al. 2009; Nomoto et al. 2006). Equation (1) leads to $f = 0.048$. The frequency of ECSNe relative to all CCSNe is thus $\sim 4\%$, assuming that all ^{86}Kr in the solar system except for a possible contribution from the s-process (18%, Arlandini et al. 1999), originates from ECSNe. This is in good agreement with the prediction from a recent synthetic model of SAGB stars (for solar metallicity models, Poelarends et al. 2008).

The remarkable difference between the 1D and 2D cases (Fig. 3) can be understood by the combined element formation in nuclear statistical equilibrium (NSE) and through the α-process (or "n-rich, α-rich freezeout from NSE", Woosley & Hoffman 1992). Representative for all elements in the normalization band of Fig. 3, the final mass fractions of the isotopes ^{64}Zn, ^{74}Ge, ^{80}Se, ^{84}Kr, ^{88}Sr, and ^{90}Zr (accounting for dominant fractions of 49%, 36%, 50%, 57%, 82%, and 51%, respectively, of their elements in the solar system, Lodders 2003) are displayed for all tracer trajectories in Fig. 4.

The α-process makes nuclei heavier than the Fe-group up to $A \sim 100$. ^{64}Zn, ^{88}Sr, and ^{90}Zr are thus produced
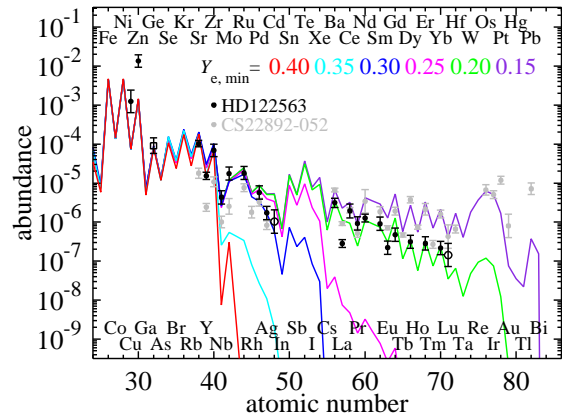

FIG. 5.— Elemental abundances for various $Y_{\text{e,min}}$ compared with the stellar abundances of the r-process deficient star HD 122563 with [Fe/H] ≈ -2.7 (Honda et al. 2006) and the r-process enhanced star CS 22892-052 with [Fe/H] ≈ -3.1 (Sneden et al. 2003). The abundances of HD 122563 and CS 22892-052 are vertically shifted to match Zr for $Y_{\text{e,min}} = 0.40$ and Ba for $Y_{\text{e,min}} = 0.15$, respectively. The Cd and Lu values in HD 122563 (open circles) are from Roederer et al. (2010), and the Ge value (open square) is from Cowan et al. (2005).

at $Y_e = 0.43$–0.49, where the α-concentration (at the end of the calculations) is $X(^4\text{He}) = 0.001$–0.1. The α-process, however, is known to leave a deep trough in the abundance curve between $A \sim 60$ and 90 because of the strong binding at $N = 28$ and 50. This explains the substantial underproduction of elements around $Z \sim 33$–37 in the 1D case (Fig. 3, blue line).

Since NSE with neutron excess ($Y_e \sim 0.4$) leads to nuclei heavier than the Fe-group up to $A \approx 84$ (see, e.g., Hartmann et al. 1985), the trough can be filled by NSE-abundances assembled in the n-rich ejecta lumps. The small $X(^4\text{He})$ ($< 10^{-5}$) at $Y_e \sim 0.40$–0.42 (Fig. 4) is indicative of the consumption of all α-particles before freeze-out from NSE. Accordingly, NSE in this Y_e-range yields substantial amounts of ^{74}Ge, ^{80}Se, and ^{84}Kr (made as ^{74}Zn, ^{80}Ge, and ^{84}Se), nuclei that cannot be created by the α-process.

In the n-rich ejecta lumps NSE-like conditions are established for several reasons. They have smaller entropies ($s \approx 13$–$15\,k_\text{B}$ per baryon) than the other ejecta (where $s \approx 15$–$20\,k_\text{B}$ per baryon; Figs. 1, 4). This favors α-particles to disappear when NSE ends as the temperature drops. In addition, the α's become easily locked up and tightly bound in nuclei, i.e., their separation energies are large (cf., e.g., Fig. 1b in Woosley & Hoffman 1992), because nuclei with n-excess do not readily release α's to move farther away from β-stability.

We find no sign of r-processing in the n-rich lumps. Our present calculations are limited to the first $\lesssim 400$ ms after bounce and do not include the neutrino-driven PNS wind. The latter, however, turned out to have proton excess in 1D models of the long-term evolution of ECSNe (Hüdepohl et al. 2010). It thus makes only p-rich isotopes with small production factors (below unity, Wanajo et al., in prep.) and has no effect on the discussed results.

4. ECSN YIELDS AND GALACTIC HALO STARS

Our results in § 3 also imply that ECSNe can be the source of Sr, Y, and Zr as observed in r-process deficient Galactic halo stars (Fig. 5). A number of such stars with detailed abundance determinations indicate, however, a

possible link with the elements beyond $N = 50$, e.g. Pd and Ag (Honda et al. 2006). Our ECSN models cannot account for the production of such elements, but in their ejecta a small change of Y_e can drastically change the nucleosynthesis (Wanajo et al. 2009). Due to limitations of the numerical resolution and the lack of the third dimension, or some sensitivity to the nuclear equation of state, it cannot be excluded that ECSNe also eject tiny amounts of matter with $Y_{e,min}$ slightly lower than predicted by the 2D simulation.

We therefore compare the nucleosynthesis for $Y_{e,min} = 0.40$ of our ECSN model and for artificially reduced values of $Y_{e,min} = 0.35, 0.30, 0.25, 0.20$, and 0.15 with the abundance patterns of representative r-process deficient (HD 122563, Honda et al. 2006) and enhanced (CS 22892-052, Sneden et al. 2003) stars (Fig. 5). For that we use the thermodynamic trajectory of the lowest Y_e (= 0.404) of the original model but apply Y_e down to 0.15 in steps of $\Delta Y_e = 0.005$. The ejecta masses in these additional Y_e-bins are chosen to be constant with $\Delta M = 2 \times 10^{-5} M_\odot$ in the cases $Y_{e,min} = 0.35$ and 0.30, and $\Delta M = 10^{-5} M_\odot$ for the other $Y_{e,min}$.

Figure 5 shows that $Y_e \lesssim 0.35$ is needed to obtain elements beyond $N = 50$. A remarkable agreement with the abundance pattern in HD 122563 up to Cd ($Z = 48$) can be seen for $Y_{e,min} = 0.30$. Such a mild reduction of $Y_{e,min}$ in the ECSN ejecta is well possible for the reasons mentioned above. A reasonable match of the heavier part beyond $Z = 48$ requires $Y_{e,min} \approx 0.20$. This, however, leads to a poor agreement for Ag and Cd. We therefore speculate that ECSNe could be the sources of the elements up to Cd in r-process deficient stars, and the heavier elements are from a different origin. Moreover, $Y_{e,min} = 0.15$ is necessary to reproduce the abundance pattern of r-process enhanced stars like CS 22892-052. Such a low Y_e seems out of reach and disfavors ECSNe as production sites of heavy r-process nuclei.

We note that the neutron-capture reactions start from seeds with $A \sim 80$ formed in NSE-like conditions (§ 3), not from the α-processed seeds ($A \sim 90$–100). We therefore prefer to call the described process producing the elements beyond $N = 50$, presumably up to Cd, "weak r-process" (Wanajo & Ishimaru 2006; Honda et al. 2006) rather than α-process or charged-particle process (Woosley & Hoffman 1992; Qian & Wasserburg 2008).

5. SUMMARY AND OUTLOOK

Using ejecta-mass tracers from a self-consistent 2D explosion model we computed the nucleosynthesis of EC-SNe. Because of a brief phase of convective overturn and the very fast explosion that is characteristic of O-Ne-Mg cores, n-rich lumps with Y_e down to 0.4 are ejected. These allow for a sizable production of the elements from Zn to Zr in NSE and by the α-process. The model yields Ge, Sr, Y, and Zr in very good agreement with abundances of r-process deficient Galactic halo stars. A mild reduction of the minimum Y_e to $\sim$0.30–0.35, which cannot be excluded due to limited numerical resolution and the lack of the third dimension, leads to a weak r-process up to the silver region (Pd, Ag, and Cd), again well matching these elements in r-process deficient stars. The formation of heavy r-process nuclei requires Y_e to be as low as $\sim$0.15–0.20 and seems out of reach for our models.

We therefore determine ECSNe as an important source of Zn, Ge, As, Se, Br, Kr, Rb, Sr, Y, and Zr in the solar system and the early Galaxy. Our models, however, underproduce Ga, which suggests the s-process as the origin of this element. The frequency of ECSNe is thus constrained to $\sim$4% of all CCSN events on average over the Galactic history, but could have been higher at early Galactic epochs, compatible with the commonality of r-process deficient halo stars.

Future better resolved and in particular 3D models will have to elucidate the role of ECSNe as site of the weak r-process. Also important are new abundance studies of r-process deficient stars for more complete information on the elements from Zn to Zr and on weak r-process products between Nb and Cd.

REFERENCES

Arcones, A. & Montes, F. 2010, submitted to ApJ; arXiv1007.1275
Arlandini, C., Käppeler, F., Wisshak, K., Gallino, R., Lugaro, M., Busso, M., Straniero, O. 1999, ApJ, 525, 886
Cowan, J. J., et al. 2005, ApJ, 627, 238
Dessart, L., Burrows, A., Ott, C. D., Livne, E., Yoon, S.-C., & Langer, N. 2006, ApJ, 644, 1063
Hartmann, D., Woosley, S. E., & El Eid, M. F. 1985, ApJ, 297, 837
Hillebrandt, W., Nomoto, K., & Wolff, G. 1984, A&A, 133, 175
Hoffman, R. D., Müller, B., & Janka, H.-T. 2008, ApJ, 676, L127
Honda, S., Aoki, W., Ishimaru, Y., Wanajo, S., & Ryan, S. G. 2006, ApJ, 643, 1180
Hüdepohl, L., Müller, B., Janka, H.-Th., Marek, A., Raffelt, G. G 2010, Phys. Rev. Lett., 104, 251101
Ishimaru, Y. & Wanajo, S. 1999, ApJ, 511, L33
Janka, H.-Th., Müller, B., Kitaura, F. S., & Buras, R. 2008, A&A, 485, 199
Johnson, A. J. & Bolte. M. 2002, ApJ, 616
Kitaura, F. S., Janka, H.-Th., & Hillebrandt, W. 2006, A&A, 450, 345
Lattimer, J. M., & Swesty, F. D. 1991, Nucl. Phys. A, 535, 331

Lodders, K. 2003, ApJ, 591, 1220
Müller, B., Janka, H.-Th., & Dimmelmeier, H. 2010, ApJS, 189, 104
Ning, H., Qian, Y. -Z., & Meyer, B. S. 2007, ApJ, 667, L159
Nomoto, K. 1987, ApJ, 322, 206
Nomoto, K., Tominaga, N., Umeda, H., Kobayashi, C., & Maeda, K. 2006, Nucl. Phys. A, 777, 424
Poelarends, A. J. T., Herwig, F., Langer, N., & Heger, A. 2008, ApJ, 675, 614
Qian, Y. -Z. & Wasserburg, G. J. 2008, ApJ, 687, 272
Roederer, I. U., Sneden, C., Lawler, J. E., & Cowan, J. J. 2010, ApJ, 714, L123
Sneden, C., et al. 2003, ApJ, 591, 936
Travaglio, C., Gallino, R., Arnone, E., Cowan, J., Jordan, F., & Sneden, C. 2004, ApJ, 601, 864
Wanajo, S., Tamamura, M., Itoh, N., Nomoto, K., Ishimaru, Y., Beers, T. C., & Nozawa, S. 2003, ApJ, 593, 968
Wanajo, S. & Ishimaru, I. 2006, Nucl. Phys. A, 777, 676
Wanajo, S., Nomoto, K., Janka, H.-T., Kitaura, F. S., Müller, B. 2009, ApJ, 695, 208
Woosley, S. E. & Hoffman, R. D. 1992, ApJ, 395, 202